SMALL-SIGNAL MODEL OF RESONANT LINK CONVERTER

Miro Milanovič[1] and Robert Kovačič[2]

[1]Faculty of Electrical Engineering and Computer Sciences, University of Maribor, Maribor, Slovenia
[2]IPS d.o.o., Research and Design Department, Ljubljana, Slovenia

Key words: power supplies, high frequency power converters, resonant link, soft switching, modeling

Abstract: The conventional small signal modeling techniques as are state space averaging and injecting-absorbed current method are not appropriate for using in converters based on high frequency resonant link (HFRL). The mentioned methods are appropriate for processes where the switching frequency is constant. Because the operation frequency of the HFRL converters is load dependent the other way of modeling must be used. In this paper a small-signal model of the HFRL converter, operating with a variable resonant link frequency, is developed by using of the estimator for linear system (ELIS) which exists under MATLAB. The high frequency resonant link voltage is modulated by the low frequency signal. The Levenberg-Marguardt aproximation method is used for evaluation of the magnitude and phase of the envelope of the high frequency resonant link voltage.

Malosignalni model pretvornika z resonančnim povezovalnim krogom

Ključne besede: napajanje elektronskih vezij, visokofrekvenčni pretvorniki, resonančni povezovalni krog, mehko preklapljanje, modeliranje

Izvleček: Običajne tehnike za malo-signalno modeliranje, kot so povprečenje v prostoru stanj in metoda iniciranega-absorbiranega toka, niso primerne za uporabo pri pretvornikih, ki so zasnovani na visoko-frekvenčnem povezovalnem krogu. Omenjeni metodi sta primerni v procesih, kjer je frekvenca prožilne enote konstantna. Ker je frekvenca delovanja visoko-frekvenčnega povezovalnega kroga spremenljiva v odvisnosti od bremenske upornosti, moramo uporabiti drugi način modeliranja. V tem članku bomo opisali postopek malo-signalnega modeliranja pretvornika z visoko-frekvenčnim povezovalnim krogom pri spremenljivi resonančni frekvenci. Postopek modeliranja bomo izvedli s pomočjo estimatorja za linearne sisteme (ELIS), ki deluje znotraj programskega paketa MATLAB. V ta namen bo napetost na visoko-frekvenčnem povezovalnem krogu amplitudno modulirana z nizkofrekvenčnim signalom. Za ocenitev vrednosti amplitude in faze ovojnice je uporabljena aproksimacijska Levenberg-Marguardt metoda.

1. Introduction

The term hf-ac or hf-dc resonant link converter usually denotes a circuit, whose main part is the resonant tank circuit. It is also possible to utilize the resonant links to derive energy storage and filtering functions normally obtained by the dc voltage link. Electrolytic capacitors provide low cost, high density energy storage in the dc voltage link of a voltage source inverter. However, the dc link based on electrolytic capacitors has several inherent limitations. One important drawback is the excessive switching loss and device stress which occurs during the switching interval. Introduction of a resonant or quasi-resonant operation principle into the known converter/inverter topology represents a possible solution of this problem. While this principle has been recognized for over ten years, the important advantages in avoiding switching stresses have been appreciated because the conventional hard-switched based converters suffer from the switching losses and hence cannot work at the very high frequency.

Recently, resonant ac or dc links have been studied and suggested as strong candidates for a power conversion link as it was described in /1/, /2/, /6/ and /7/. The using of high frequency ac resonant link principle for energy storage purposes enables to reduce the device losses or device stress by restricting the switching time to the instants of zero current or zero voltage. In general ac or dc high frequency link inverters have been used only for high-power application as are the motor drives, UPS etc. as it is shown in Fig. 1 (a). The converter proposed in /1/, /2/ and [6] are based on bidirectional switches.

In Fig 1 (b) is shown the converter circuit which enables to supply the resonant tank circuit only by using unidirectional switches /3/. This principle of the operation can be used in the low power dc-dc conversion as well, as it is shown in Fig. 2 (a) and (b). The energy storage function is taken over by resonant tank circuit, by using the transformer the energy can be provided to load. The load side of transformer is equiped by rectifier and filter elements. In this paper the structure of dc-dc conversion based on an ac-resonant link is presented. This resonant tank circuit is capable to provide the energy storage function instead of the conventionaly used electrolytic capacitor. The main drawbacks is that the resonant link voltage magnitude and the operation frequency of resonant link circuit is load dependent.

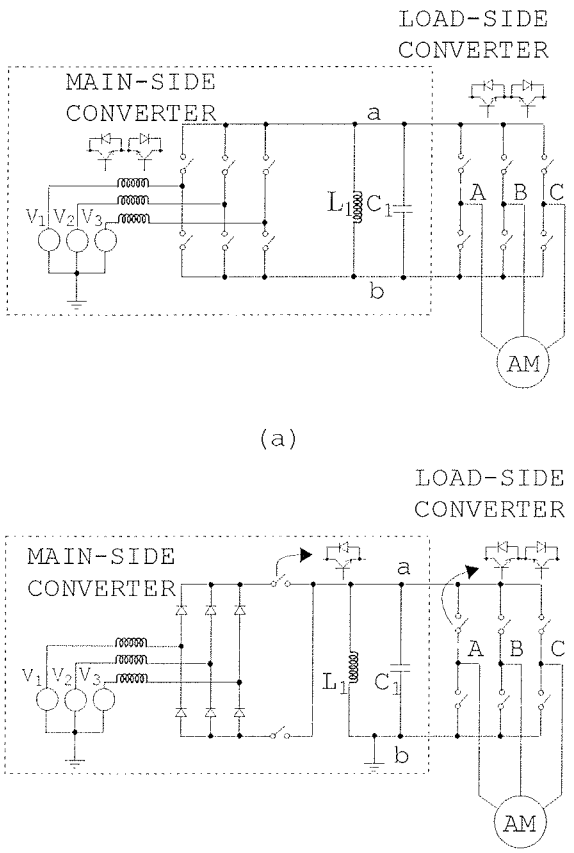

Fig.1: Induction motor drive based on resonant link converter circuit: (a) Main side converter with bi-directional switches; (b) Main side converter with uni-directional switches.

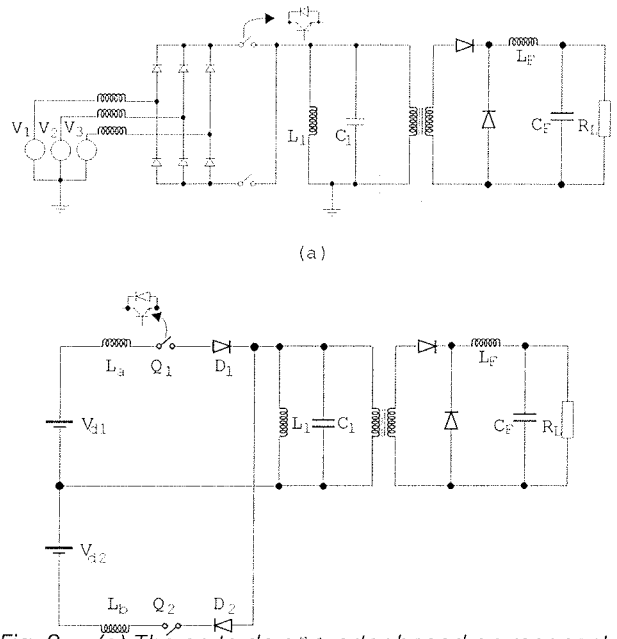

Fig. 2: (a) The ac to dc converter based on resonant link circuit (b) The dc to dc converter based on resonant link circuit.

Hence the conventional methods for the small-signal modelling as are state space averiging, injected-absorbed current method, pwm equivalent circuits /4/ cause the modelling problems because the conventional methods require the constant switching frequency of operation /8/, the method based on the measured data is proposed. The estimator for linear system (ELIS) has been used for small-signal model developing of the HFRL converter, which is operating with a variable resonant link frequency. ELIS is the software available as a toolbox in Matlab-Simulink package. The high frequency resonant link voltage is modulated by the low frequency signal. The Levenberg-Marguardt approximation procedure is used for accurate evaluation of the magnitude and phase of the HFRL voltage envelope from measured data. The control parameter adjustment will be based on developed small signal model.

2. Principle of the operation

The basic scheme for "evolution" of the dc to ac high frequency converter circuits is shown in Fig. 3. In steady state the parallel resonant circuit consists of L_1 and C_1 operates and provides the energy to the resistor R_L (R_L represents the load). Transistor Q_1 could be switched on when the voltage on the parallel resonant link crosses zero as it is shown in Fig. 4 (time instant t_0). Then L_a with the elements of parallel resonant tank circuits L_1 and C_1 establish a series resonant circuit. The current through transistor Q_1 is supposed to be of sinusoidal wave shape (interval A). When the current through Q_1 crosses zero, diode D_1 turns off and transistor Q_1 can be turned off as well (time instant t_1). When the series resonant frequency ω_s is higher than parallel resonant frequency ω_p the soft switch operation of converter has been used. The energy was provided from dc voltage source V_{d1} to parallel tank circuit during the time interval A. Because of similarity with half-wave operation of diode rectifier the circuit can be described as "half-wave" configuration of the dc-ac hf resonant link converter.

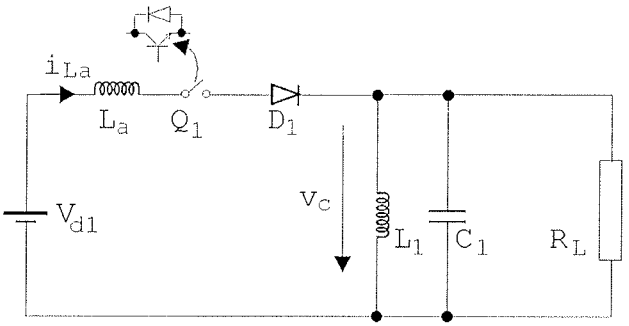

Fig. 3: The "half-wave" topology of dc-ac hf resonant link converter.

Operation of the circuits from Figs. 5 (a) and (b) is similar. The energy is provided from the dc-supply to the parallel resonant tank circuit in both half periods of the output ac high frequency resonant link voltage. Because of that the circuit could be titled a "full-wave" configuration of the ac-

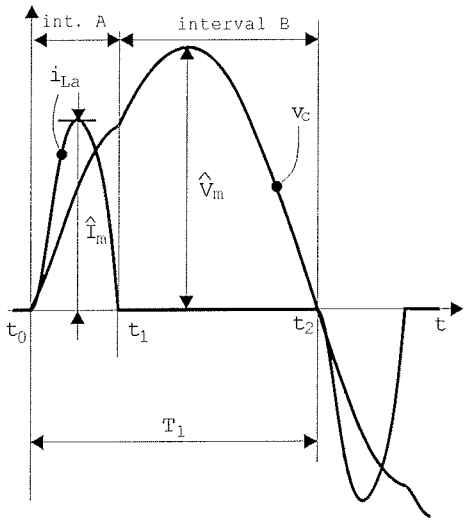

Fig. 4: (a) The current and voltage wave-shape.

hf resonant link converter. The oscilograms measured in the "full-wave" configuration are shown in Fig. 4 (b). In order to provide the energy from main supply to the resonant tank circuit the configurations shown in Figs. 6 (a) and (b) are suggested. The circuit in Fig. 6 (a) is coming as evolution of the circuit shown in Fig. 5 (a). The disadvantages of this circuit are two capacitors, which "simulate" the voltage sources V_{d1} and V_{d2} and there are still two inductors L_a and L_b and two diodes D_1 and D_2.The component minimized converter circuit is shown in Fig. 6 (b). The converter consists of diode bridge, the transistor bridge, inductor L_a and the resonant tank circuit. The function of two series diodes D_1 and D_2 can be taken over by diodes from the rectifier bridge.

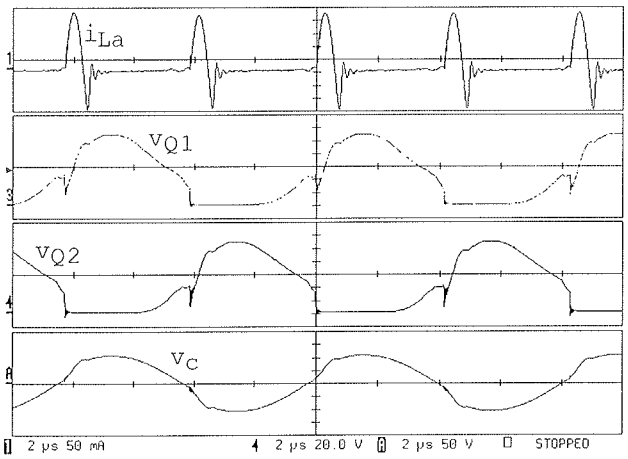

Fig. 4: (b) Experimental results measured in "full-wave" configuration

3. The small signal modeling

The hard switch converters represent the non-linear circuits and because of that it's analysis is so complicated. Because the load, connected at the converter output, requires constant voltage regardless of the current, a voltage controller circuit should be implemented. Many algorithms are developed for the linear time invariant circuits, which can be described in "s" or "z" space. Because of that the linearization method as are the state space averaging, injection-absorbed current method and etc. are widely used. Sometime the modeling process is of great pretension because of non-ideal and parasitic elements. In this case the transfer function, which is necessary for controller parameter design, could be measured.

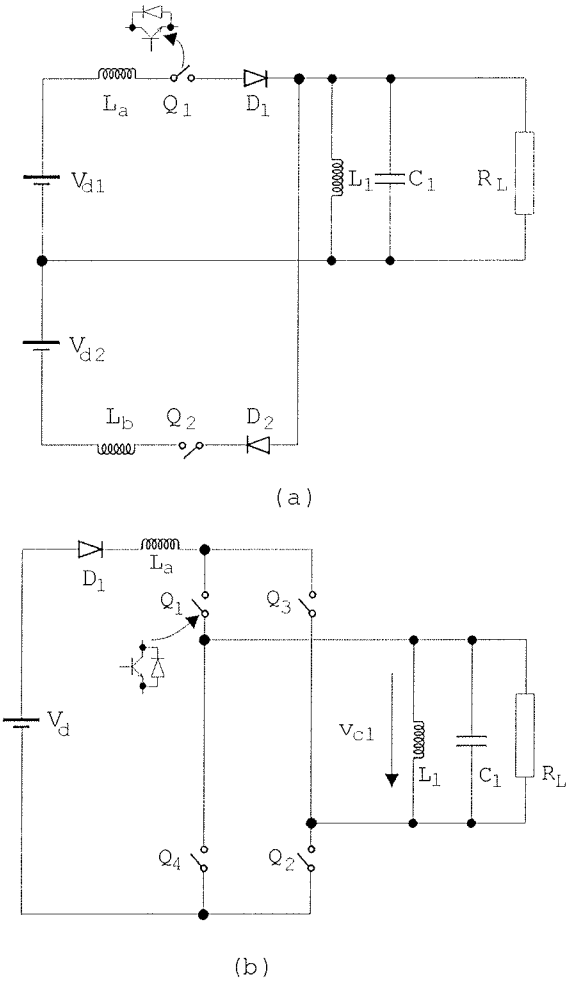

Fig. 5: (a) The "full-wave" topology of dc-ac hf resonant link converter. (b) The "bridge" topology of dc-ac hf resonant link converter.

3.1 The standard procedure for measuring of small signal model

The small-signal model of the converters can be evaluated through the frequency response (FR) of the circuit. The FR of the circuit may be regarded as a complete description of the sinusoidal steady-state behavior of a circuit as a function of the frequency. In Fig. 7 (a) the standard open loop procedure of FR measurement for buck converter is shown. The "small" signal v_{ref} is adding to dc voltage V_{DC}, which defines the steady state of the converter operating points. The large gain of the object causes that the steady

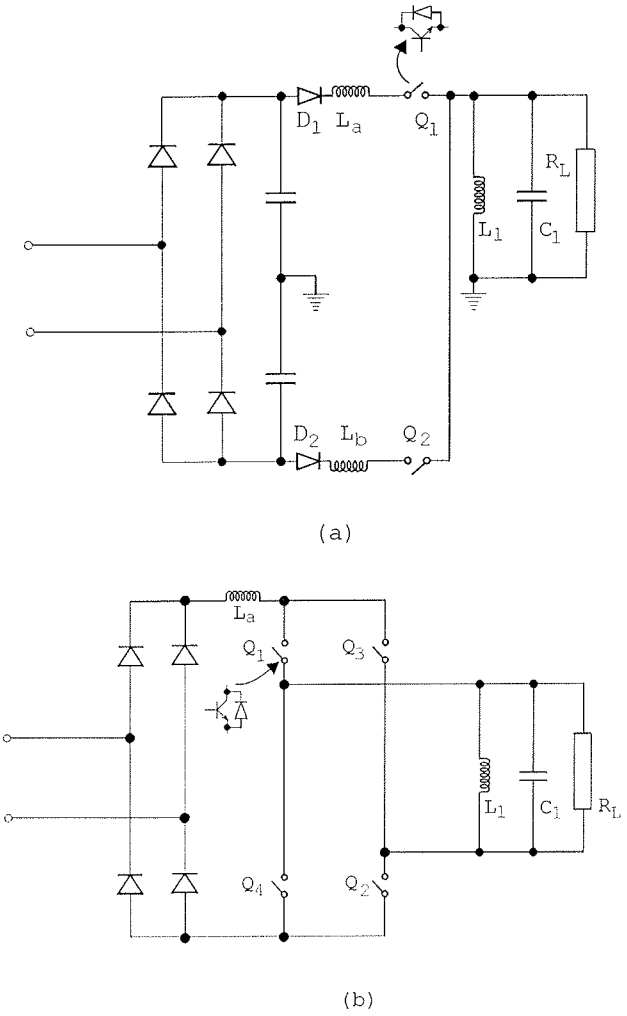

Fig. 6: (a) the "full-wave" topology of dc-ac hf resonant link converter connected with the mains. (b) The "bridge" topology of dc-ac hf resonant link converter connected with the mains.

state is unstable, therefore the small signal perturbation causes the large changing of the output voltage. For example when the gain is 60 *dB* (i. e. 1000) the input small signal perturbation of 1 *mV* will cause the output changing of 1 *V*. Through the measurement process the different operating points of the power stage are exited and such measured frequency response is not accurate. How to avoid this problem is described in /10/. Network analyzers could measure the control objects with large gain where the small signal perturbation has been injected into closed control loop as it is shown in Fig. 7(b). During the measurement process the controller keeps the converter operating point stable. The measurement of the converter FR is very accurate when the network analyzer was used. The ac output has been measured by narrow pass-band filter, which guaranties good disturbance rejection. These instruments also repeat measurement procedure by equal frequency and as result; the arithmetic average value of the FR at the particular frequency is evaluated.

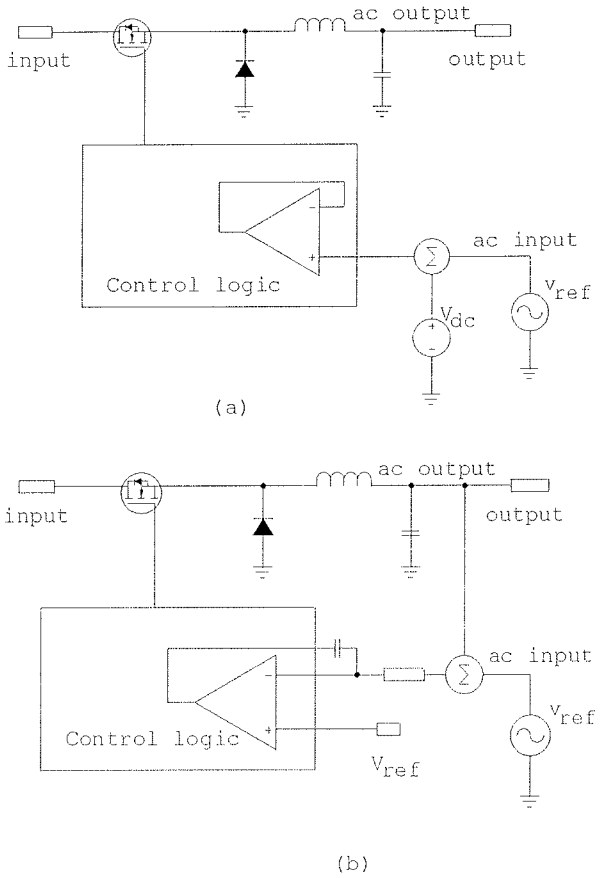

Fig. 7: (a) The buck converter open loop measurement of the frequency response; (b) The buck converter closed loop measurement of the frequency response.

3.2 The measurement procedure for small signal model of HFRL converter

The ac-hf resonant link converter does not have such "nice" properties. The output link voltage is alternative and when small signal perturbation is injected the amplitude modulation will appear on link voltage. The resonant link voltage is alternative but not sinusoidal as it is shown in Fig. 4 (a) and (b). The amplitude changing caused by input small signal perturbation is sinusoidal. The measurement circuit is shown in Fig. 8.

The open-loop principle has been used. This could be used because the open loop gain was only 40 *dB*. The small signal voltage v_{in} and output signal on transistor Q_2, the voltage v_c has been measured by scope *LC334A*. In Fig. 9 the measurement results are shown.

The results shown in Fig. 9 were also available as a file in binary form. This data has been processing with Mathematica, where the Levenberg-Marquardt method for approximation was used to find the unknown parameters of the signal described by (1). Both the input signal v_{in} and the envelope of the output signal v_c could be defined with expression:

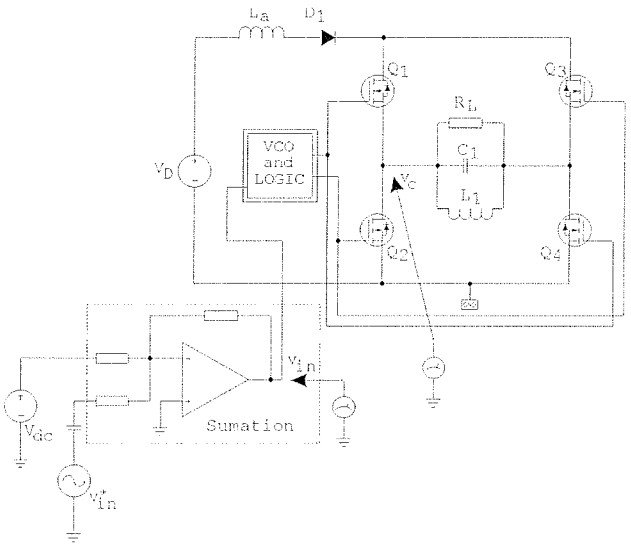

Fig. 8: The open loop circuit for FR measurement of the HFRL converter

$$v_x = V_{DXx} + \hat{V}_x \cos(\omega t + \varphi) \qquad (1)$$

where V_{DXx} is the dc operating points, $\hat{V}_x$ represents the magnitude of the input signal or magnitude of the output signal envelope, ω is the signal frequency and φ is the phase angle regarding scope synchronization point.

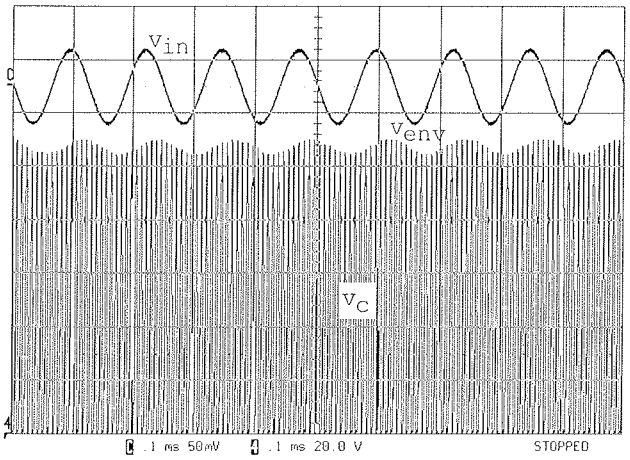

Fig. 9. Measurement results of the input voltage v_{in} and output voltage v_c

From the difference between input phase angle and output phase angle the phase diagram of the HFRL converter could be evaluated as well. Fig. 10 (a) shows the input signal waveform (green) with measurement noise and the solid line is the result of approximation by Levenberg-Marquardt method. The output signal causes some problems because it has been defined as peak values of the resonant link voltage and these points are discrete. The result of this approximation is shown in Fig. 10 (b). From this results all parameters needed in (1) have been defined and the measurement data becomes appropriate for evaluation of the gain and phase waveforms in frequency domain.

By using the estimator for linear system (ELIS) which exists under the Malab the converter model has been derived. The ELIS works better with a set of the measured data, which are measured under the same conditions as shown in Table 1.

To identify the model of the converter a general presumption, i.e. the number of zeros and poles must be defined.

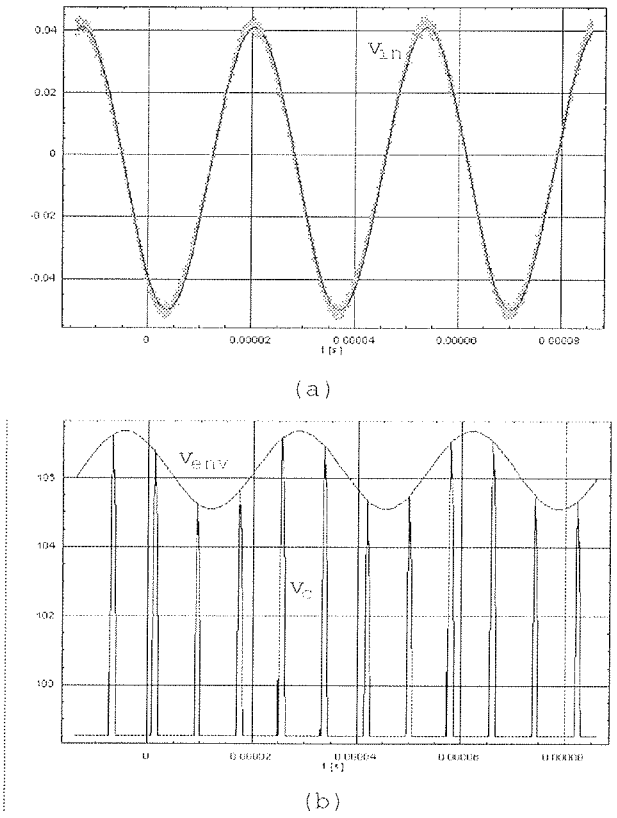

Fig. 10. Measurement results of the input voltage v_{in} and output voltage v_c

In Table 2 the placement of the poles as a result of the evaluation procedure by ELIS is shown. In the first and second columns the evaluation results of the first and third order system are presented. In the third and fourth columns the models of the first order system with the different delays have been shown /5/. When the number of poles has been changed the placement of one of the poles did not change significantly. In the third order model this pole has a natural frequency of 42644 *rd/s*. Two other poles have complex values.

There exists a physical explanation of this natural frequency. The paramount of interest is not the dynamics of the tank circuit itself but the dynamics of the resonant link voltage envelope $\tilde{v}_{env}$ caused by the input voltage $\tilde{v}_{in}(s)$. For $\tilde{v}_{env}$ dynamics could be supposed it is dependent on resistance R_L and capacitance C_P. For chosen R_L and C_P (R_L=23706Ω, C_P=2.014*nF*) the natural frequency of this parallel system is $\omega_{RC} = 1/R_L C_P = 20946$ *rad/s* which is more or less half of the previous derived natural frequency (Table 2).

Table I: Measurement results

	1. experiment		2. experiment		3. experiment	
Freq. *f(Hz)*	Gain *A(dB)*	Phase φ(*deg.*)	Gain *A(dB)*	Phase φ(*deg.*)	Gain *A(dB)*	Phase φ(*deg.*)
200	40.835	-3.0271	40.2397	-2.46356	40.4445	-3.54746
500	41.2899	-4.20871	40.2185	-2.65827	40.1483	-3.10764
800	41.3075	-6.54668	40.1752	-5.17673	40.0429	-4.50148
1000	41.2422	-8.0458	39.9262	-5.29607	40.0305	-3.88876
2000	41.1928	-17.02	39.921	-13.6055	39.9932	-15.9025
3000	40.5761	-25.7001	39.6663	-23.8292	39.6571	-23.6579
5000	39.4706	-40.5851	38.6214	-37.1977	38.691	-38.2392
8000	37.389	-56.2334	36.7191	-53.3234	36.6696	-54.2372
10000	35.842	-64.4906	35.374	-61.4672	35.3644	-61.0895
20000	31.3755	-84.3958	30.8801	-84.5519	30.8145	-82.9609
30000	28.5177	-95.866	28.0225	-98.1729	28.4572	-97.4357

Table II: Pole placement

	1st model	2nd model	3rd model	4th model
Number of zeros	0	0	0	0
Number of poles	1	3	1	1
delay	0	0	1.8μs	1.9μs
The values of poles	-3698	-42644	-44729	-45106
		- 194816 +j445496		
		- 194816 -j445496		

That's why the pole placement could be expressed as:

$$s_1 = -2\omega_{RC} \tag{2}$$

Two complex poles appear in the system because of the discrete nature of the link voltage (only peak of the HFRLV has been observed) and the discrete VCO controlled modulator. The steady state operation frequency ω was $1.6\text{x}10^6$ rd/s (cca. 250*kHz*). The authors in /4/ and /5/ suggest that the discrete structure of such system could be described by time delay as it follows:

$$H(s) = \exp(-sT_d) = \frac{1}{1 + sT_d + \frac{1}{2}sT_d^2 + \ldots} \tag{3}$$

where T_d is half of the period of the resonant link voltage. The gain of the plant can be estimated from the energy stored in the capacitors and dissipated on the load resistor. The magnitude of the current through L_a and the time t_{on} as difference of t_1 and t_0 can be evaluated by formulas:

$$\hat{I}_m = -\frac{i_{L1}(0)L_1}{L_1 + L_a} + \sqrt{\left(\frac{i_{L1}(0)L_1}{L_1 + L_a}\right)^2 + \left(\frac{V_{d1}L_1}{L_1L_a + L_a^2\omega_s}\right)^2} \tag{4}$$

$$t_{on} = \frac{\pi}{\omega_s} - 2\frac{i_{L1}(0)L_1}{L_1 + L_a} \frac{1}{\omega_s\sqrt{\left(\frac{i_{L1}(0)L_1}{L_1 + L_a}\right)^2 + \left(\frac{V_{d1}L_1}{L_1L_a + L_a^2\omega_s}\right)^2}} \tag{5}$$

where:

$$\omega_s = \frac{1}{\sqrt{L_nC_1}}, \qquad L_n = \frac{L_1L_a}{L_1 + L_a}$$

The average value of the current through La in half-period of the resonant link voltage is obtained as

$$I_{La,avg} = \frac{\hat{I}_m t_{on}}{\pi T_1} \tag{6}$$

The energy provided inside whole period is obtained by:

$$W = 4V_{d1}I_{La,avg}T_1 \tag{7}$$

Presume that the resonant link voltage has sinusoidal waveshape, than its rms value is:

$$V_{c,ms} = \sqrt{\frac{WR_L}{2T_1}} \tag{8}$$

and magnitude:

$$\hat{V}_m = \sqrt{2}V_{c,ms} = \sqrt{\frac{WR_L}{T_1}} \tag{9}$$

where ^ represents the magnitude of the current or voltage. The gain consists of the gain of VCO (K_{VCO}) and the converter gain K_Uw which is frequency dependent /3/. By substitution (4)-(8) into (9) the slope could be expressed as:

$$K_{u\omega} = \frac{\partial \hat{V}_c}{\partial \omega_p} = \hat{I}_{La}\sqrt{L_a R_L/\pi}\ \left(2\sqrt{\omega_p}\right)^{-1} \qquad (10)$$

Therefore the whole transfer function is:

$$\frac{V_{env}}{V_{in}} \cong \frac{K_{VCO}K_{u\omega}}{2\omega_{RC}\left(1+\frac{s}{2\omega_{RC}}\right)\left(1+T_d s+\frac{1}{2}T_d^2 s^2\right)} \qquad (11)$$

In Figs. 11 the different frequency responses are shown ("+" is the average value of the measured results from Table 1).

3.3 The control of HFRL converter

In this section the experimental results obtained on a bridge structure of the HFRL converter are shown. The control problem can be defined as a necessity to keep constant magnitude of ac-hf resonant link voltage regardless of load conditions. For small-signal modeling the above-described method has been used. In lab. prototype the measurement is realized by using the appropriate electronics circuit as it is shown in Fig. 12. The control object includes the voltage-controlled oscillator as modulator (VCO), dc-ac high frequency converter and sample and hold circuit (S/H) as a peak voltage detector. Fully analog circuits generate the control signals. For triggering units (instead of pwm) the VCO has been used. The S/H circuit is used for the measurement of the peak of the high frequency voltage. The capacitor current i_{C1} has a delay with respect to voltage v_C of exactly $\pi/2$. If the voltage is sampled in this time instant (when the current i_{C1} crosses zero), the peak value of voltage v_C will be measured. This simple phenomenon eliminates the need for filter in measuring circuit. Based on the developed small signal model the PI controller has been designed. In Fig. 13 the experimental results are shown. In particular time instant the load resistance has been changed which has influence on the high frequency resonant link voltage v_c. From the waveforms it is evident that the control of the high frequency resonant link voltage v_c has been reached.

4. Conclusion

The high frequency resonant link converter has been discussed in this paper. The energy has been provided to the resonant tank circuit through the series resonant process. Because of that the soft switch converter operation has been reached. The main effort has been done at the efficiency study and consequently the efficiency increases up to 92%. The magnitude of the resonant link voltage is always larger than the dc input voltage. This "disadvantage" can be avoided by introducing the transformers and the lower voltage can be reached at the converter dc output. The EMI influences is lower than the hard switch converter usually produces because the current and voltages have sinusoidal wave-shape and because of soft switching operation.

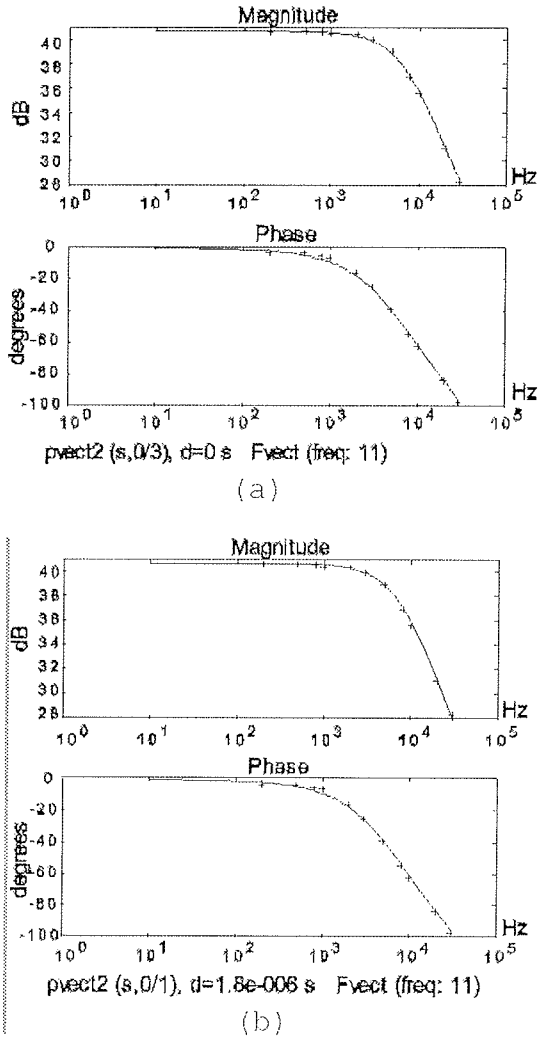

Fig. 11: (i) Frequency response (number of zeros are 0, number of poles are 3, delay is 0μs; (ii) Frequency response (number of zeros are 0, number of poles are 1, delay is 1.8μs)

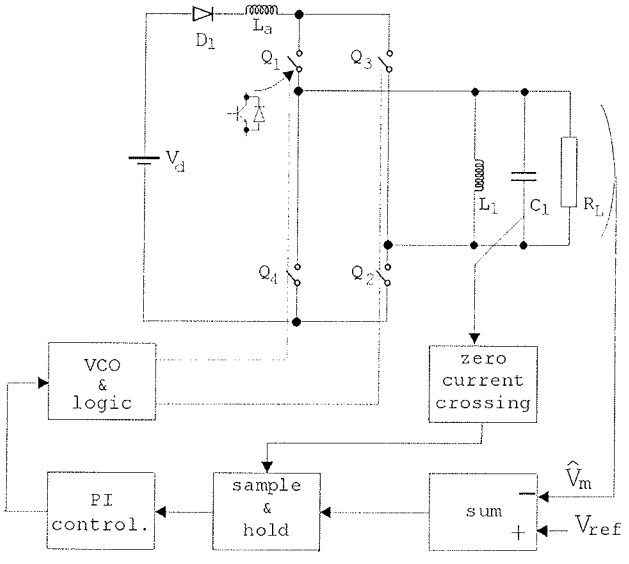

Fig. 12: The control sheme of HFRL converter

For control purposes the method based on measurement data has been used. The MATLAB tool-books ELIS for identification of the small signal model of the ac resonant link converter has been investigated. For accurate identification of resonant link voltage parameters (i. e. magnitude and phase of the voltage envelope) the Levenberg-Marguardt method was used. The experimental results have shown that this procedure is capable of providing a good solution of the frequency response for the non-linear problem. Based on this modeling the control of HFRL voltage has been realized.

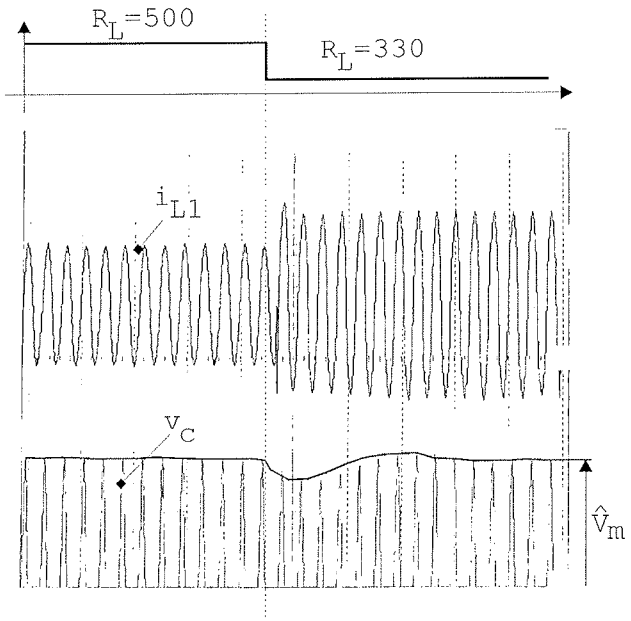

Fig.13: Experimental results when the load resistance has been changed: (uper) the current of parallel resonant link circuit i_{L1} (200 mA/div), (lower) the magnitude of resonant link voltage v_c (20V/div).

References

/1/ SOOD, P. K., LIPO, T. A.,' Power conversion distribution system using a resonant high frequency AC-link', *IEEE Transactions on Industry Applic.* 1988, 24, (2) pp. 586-596.

/2/ DIVAN. D. M., 'The resonant DC-link converter - a new concept in static power conversion', *IEEE Transactions on Industry Applic.* 1989, 25, (2) pp. 317-325.

/3/ MILANOVIC, M., KOVACIC R., MIHALIC F. and BABIC R. 'The control of an AC to HF-AC resonant link converter', *Inf. MIDEM, 1996,* 26, (1), pp. 7-13.

/4/ KISLOVSKI, A. S., REDL, R., SOKAL, N. O., 'Dynamic Analysis of Switching-Mode DC/DC Converters' Van Nostrand Reinhold, New York, 1991.

/5/ TSAKHURUK, T. A., LEHMAN, B., STANKO-VIC, A. M., TADMOR, G., 'Effects of Finite Switching Frequency and Delay on PWM Controlled Systems', *IEEE Transactions on Circuits and System, Fundamental theory and Application,* vol. 47, No.4 pp. 555-567, April 2000.

/6/ S.K.SUL, T.A.LIPO, 'Design and performance of a high frequency link induction motor drive operating at unity power factor', *IEEE IAS Annual Meeting*, Proc., pp. 308-313, Oct. 1988

/7/ Y. MURAI, S. MOCHIZUI, P. CALDERIA, T.A.LIPO, 'Current pulse control of high frequency series resonant dc link power converter', *IEEE IAS Annual Meeting*, Proc., pp. 1023-1030, Oct. 1989.

/8/ J. HOLTZ, 'Pulsewidth modulation - a survey', *IEEE Transaction on Industrial Electronics*, vol.39, No.5, pp, 410-420, October 1992.

/9/ M. MILANOVIC, F. MIHALIC, D. MARKO, K. JEZERNIK, 'The ac to hf/ac resonant link converter' *IEEE PESC Conf. Rec*, pp. II/750-756, 1995.

/10/ R. LENK, 'Practical design of power suppliesr' Van Nostrand Reinhold, New York, 1992.

Dr. Miro Milanovič, univ.dipl.ing.
Univerza v Mariboru
Inštitut za avtomatiko in robotiko
Fakulteta za elektrotehniko,
računalništvo in informatiko
Smetanova 17, Maribor, Slovenija
e-mail: milanovic@uni-mb.si

mag. Robert Kovačič, univ.dipl.ing.
IPS d.o.o., Research
and Design Department
Cesta Ljubljanske brigade 17, Ljubljana, Slovenia
e-mail: kovacic@ips.si

Prispelo (Arrived): 30.05.2002 *Sprejeto (Accepted): 25.03.2003*